JOURNAL OF APPLIED PHYSICS VOLUME 91, NUMBER 10 15 MAY 2002

Ru_xCr_{1-x}/Ta underlayer for Co-alloy perpendicular magnetic recording

K. W. Wierman,[a] T. J. Klemmer, B. Lu, G. Ju, and K. J. Howard
Seagate Research, 2403 Sidney Street, Pittsburgh, Pennsylvania 15203-2116

A. G. Roy and D. E. Laughlin
Data Storage Systems Center, Carnegie Mellon University, Pittsburgh, Pennsylvania 15213

The effects of the Ru_xCr_{1-x}/Ta underlayer on the microstructural and magnetic properties of CoCrPtB perpendicular films were investigated. The hcp Ru_xCr_{1-x} (0002) texture was observed to grow perpendicular to the film plane with narrow rocking curves of 2°–3°. High-resolution transmission electron microscopy indicated epitaxial growth of the CoCrPtB on top of the Ru_xCr_{1-x}/Ta underlayer. In-plane x-ray diffraction scans indicate that as the Cr atomic composition increases in the Ru_xCr_{1-x} underlayer, the a-lattice parameter was found to contract more closely matching the CoCrPtB a-lattice parameter [measured with $(11\bar{2}0)$]. In addition, the rocking curves for the CoCrPtB (0002)-texture induced by the (0002) textured Ru_xCr_{1-x} buffer showed narrowing peaks (4.5°–3.5°) as the Cr concentration increased from 0% to 40%. [DOI: 10.1063/1.1447498]

I. INTRODUCTION

Perpendicular magnetic recording has the potential to achieve recording densities well beyond 100 Gb/in^2 areal density.[1] Underlayers to enhance the Co (0002) texture growth perpendicular to the film plane are required to achieve thin Co-alloy layers with good perpendicular anisotropy.[2] Underlayers with hcp structures, principally Ti, have been demonstrated as a means to enhance the growth of hcp Co (0002) texture.[3,4] Often an amorphous-like transition region forms due to a high elastic strain energy in the initial growth of the Co alloy induced by a large a-lattice mismatch between the underlayer and Co alloy.[5] Ru underlayers grown on freshly cleaved mica substrates by electron-beam evaporation is shown to grow epitaxially CoCr (0002) with narrow rocking curves.[6] Transmission electron microscopy (TEM) image of $CoCr_{19}Pt_{10}$ grown on a $CoCr_{25}Ru_{25}/TiCr_{10}$ underlayer was shown to provide a good epitaxially match.[7] In this study Ru_xCr_{1-x}/Ta underlayers grown on amorphous Si/SiO_2 substrates and the effects on the microstructural and magnetic properties of CoCrPtB perpendicular films were investigated. Cr is added to Ru to further reduce the a-lattice parameter to provide a better lattice match with the CoCrPtB and enhance the (0002) texture.

II. EXPERIMENT

The CoCrPtB and Ru_xCr_{1-x} films were deposited by a dc magnetron sputtering system with base pressure of 5×10^{-9} Torr. The Ru_xCr_{1-x} underlayers were cosputtered from pure Ru and Cr targets. The CoCrPtB films were deposited directly from an alloy target. The substrates were 3 in. Si wafer coated with 100 nm thermally grown amorphous SiO_2 layer. The sputter power density of the CoCrPtB, Ta, Ru, and Cr targets was between 14 and 2 W/cm^2. The sputtering Ar pressure was 3 mTorr for the Ru_xCr_{1-x}/Ta and 5 mTorr for the CoCrPtB. Substrate temperature for the film growth was kept at 280 °C by a resistive heater. Crystallographic orientations of the thin films were studied by a Philips X'Pert x-ray diffractometer (XRD) with Cu $K\alpha$ radiation. The microstructures of the thin films were investigated by a Philips EM 420T transmission electron microscope (TEM). The magnetic properties were measured by a vibrating sample magnetometer (VSM).

III. RESULTS AND DISCUSSION

The symmetric $2\theta/\theta$ XRD spectra of the Ru_xCr_{1-x}/Ta films are shown in Fig. 1. For all Cr compositions a dominant (0002) and (0004) peaks are observed. As the Cr concentration increases there is a steady shift of both peaks to higher 2θ values. The broad peak occurring at 34° is due to the Ta underlayer. The angular dispersion of the Ru_xCr_{1-x} and the CoCrPtB (0002) orientations were investigated by

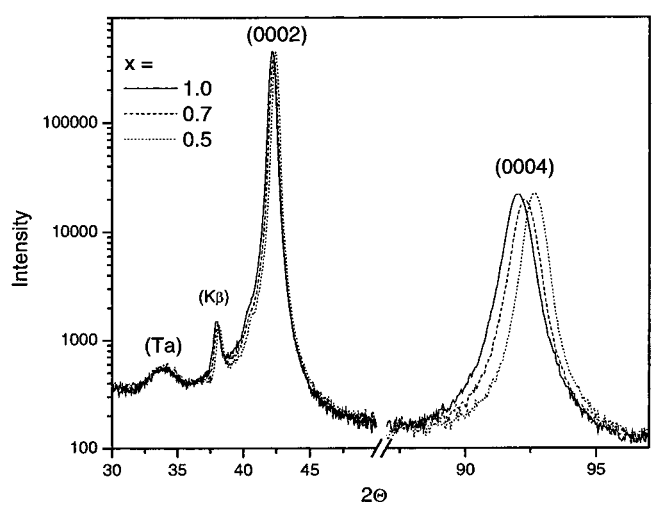

FIG. 1. $2\theta/\theta$ XRD scans of Ru_xCr_{1-x} 50 nm/Ta 5 nm with $X=100\%$, 70%, and 50%.

[a]Electronic mail: kurt.w.wierman@seagate.com

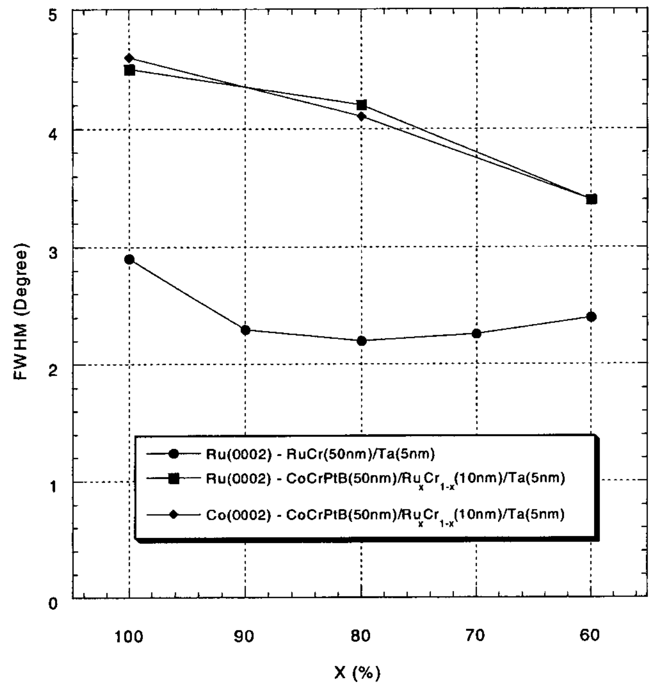

FIG. 2. Angular dispersion of (0002) Ru and Co peaks for Ru_xCr_{1-x} (50 nm)/Ta (5 nm) and CoCrPtB (50 nm)/Ru_xCr_{1-x} (10 nm)/Ta (5 nm).

rocking curves. The full width at half maximum (FWHM) results from these rocking curve scans are graphed in Fig. 2. It can be seen that both Ru_xCr_{1-x} and CoCrPtB FWHMs steadily decrease with the addition of Cr. The CoCrPtB films have rocking curves FWHM that match the Ru_xCr_{1-x} underlayer FWHM indicated that heteroepitaxial growth of the CoCrPtB is occurring.

The a-axis lattice parameter can be calculated using in-plane scans of the $(11\bar{2}0)$, see Fig. 3. The CoCrPtB maintained a constant a-axis length of 2.552 Å while the Ru_xCr_{1-x} show a shift to smaller a-axis lattice parameter with increasing Cr. The lattice misfit between CoCrPtB and Ru_xCr_{1-x} improves from 7.3% to 5.2% as the Ru composition goes from 100% to 60%. The c-axis length of the unit cell was calculated from the (0004) peak position in the $2\theta/\theta$ scan. The values of the a and c-axis lattice parameters as well as c/a ratio of the Ru_xCr_{1-x} films are listed in Table I. The decrease of the a and c lattice is nearly linear and maintains a c/a ratio near 1.58.

TABLE I. The lattice parameters of a and c axes as well as c/a ratio for Ru_xCr_{1-x}.

$X=\%$	a (Å)	c (Å)	c/a
100	2.704	4.286	1.585
90	2.704	4.277	1.582
80	2.698	4.271	1.583
70	2.694	4.263	1.583
60	2.689	4.263	1.586
50	2.684	4.263	1.588

VSM measurements on the $x=100\%$, 80%, and 60% were done on the same samples sent for TEM analysis. The normalized perpendicular hysteresis loops show a decrease in coericivity (H_c) with increasing Cr, see Fig. 4. However, measurements with the field applied in the plane of the sample showed all three samples saturating ($H_{k\ \mathrm{eff}}$) near 8.5 kOe. The magnetic moment was measured at 509, 501, and 476 emu/cm^3 for $x=100\%$, 80%, and 60% respectively. The Cr diffusion from the underlayer into the Co alloy has been reported for longitudinal media[8] and is expected to be the cause of the decrease in H_c in these materials.

High-resolution cross-sectional transmission electron micrograph (TEM) images show distinct Ru_xCr_x/CoCrPtB ($x=100\%$, 80%, and 60%) interface with continuity of the (0002) plane stacking over extensive region. Figure 5 shows a representative image for $x=60\%$. No initial amorphous like transition regions are seen in any of the images. The Ta layer contains small ($\sim 1-2$ nm) randomly oriented body-centered-tetragonal crystallites. Columnar Ru_xCr_{1-x} grains are visible originating at the Ta interface. Columnar grain diameters are 12–15 nm. Continuity of the $(10\bar{1}0)$ lattice planes across the CoCrPtB/Ru_xCr_{1-x} interface are seen in

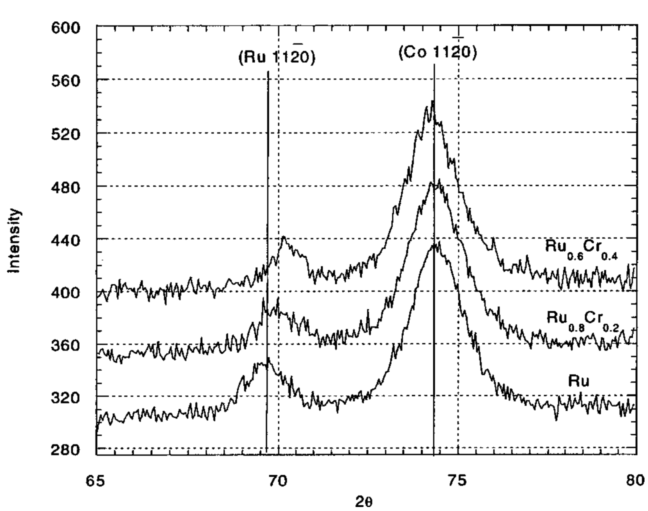

FIG. 3. In-plane XRD scans of CoCrPtB (50 nm)/Ru_xCr_{1-x} (10 nm)/Ta (5 nm) for $X=100\%$, 80%, and 60%.

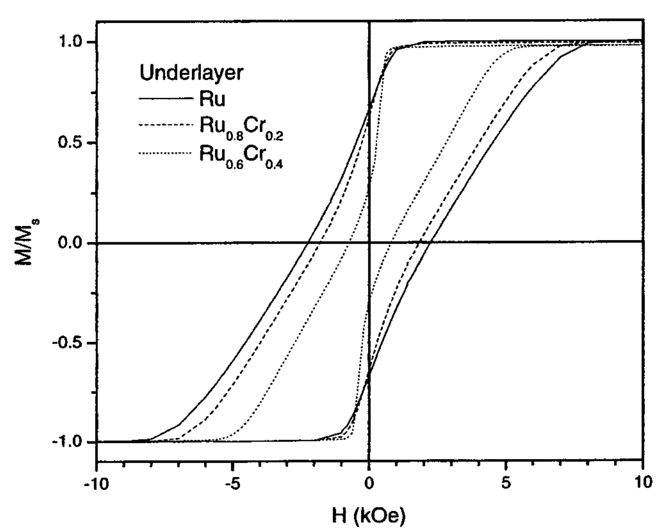

FIG. 4. Cross-sectional TEM image of Ta CoCrPtB (50 nm)/$Ru_{0.6}Cr_{0.4}$ (10 nm)/Ta (5 nm) sample.

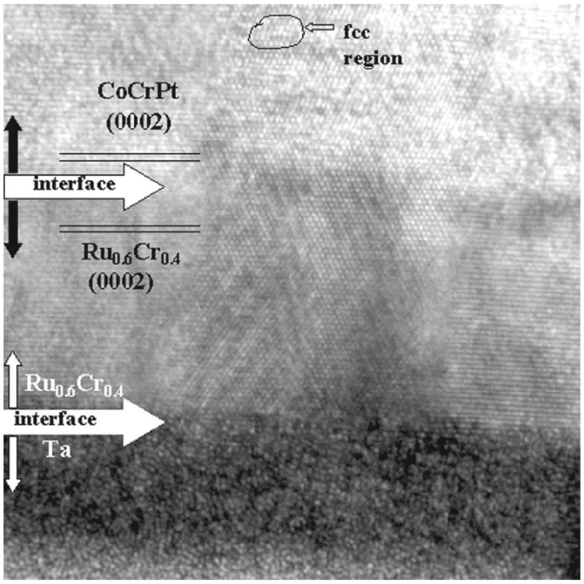

FIG. 5. Perpendicular VSM hysteresis loops of CoCrPtB (50 nm)/Ru_xCr_{1-x} (10 nm)/Ta (5 nm) for $X = 100\%$, 80%, and 60%.

individual growth columns. The grains extend up through the CoCrPt layer, although interruptions in the desired hcp stacking are visible.

IV. CONCLUSION

Adding up to 40% of Cr to the Ru_xCr_{1-x}/Ta underlayers has been shown to reduce the angular dispersion in the (0002) texture. Heteroepitaxial growth of CoCrPtB layers as then successfully achieved on the Ta/Ru_xCr_{1-x} seed layer The heteroepitaxial relationships have been confirmed by XRD and TEM. Improved c-axis anglar dispersion of (0002) CoCrPtB magnetic layers was observed as the Cr concentration was increased from 0% to 40%. Stacking faults were observed in the hcp CoCrPtB thin films deposited onto all Ru_xCr_{1-x} underlayers.

[1] H. N. Bertram and M. Williams, IEEE Trans. Magn. **36**, 4 (2000).
[2] S. Iwasaki, K. Ouchi, and N. Honda, IEEE Trans. Magn. **16**, 1111 (1980).
[3] M. Futamoto, Y. Honda, and H. Kakibayashi, IEEE Trans. Magn. **21**, 1426 (1985).
[4] Q. Kitakami, Y. Ogawa, H. Fujiwara, F. Kugiya, and M. Suzuki, IEEE Trans. Magn. **25**, 2607 (1989).
[5] I. S. Lee, H. Ryu, J. J. Lee, and T. D. Lee, J. Appl. Phys. **85**, 6133 (1999).
[6] K. Krishnan, T. Takeuchi, Y. Hirayama, and M. Futamoto, IEEE Trans. Magn. **30**, 5115 (1994).
[7] Y. Hirayama, A. Kikukawa, Y. Honda, N. Shimizu, and M. Futamoto, IEEE Trans. Magn. **36**, 2397 (2000).
[8] M. Sato, Y. Onishi, and A. Nakaue, IEEE Trans. Magn. **29**, 3685 (1993).